

ChemComm

Accepted Manuscript



This article can be cited before page numbers have been issued, to do this please use: X. Tan, Y. Sun, T. Sun and H. Zhang, *Chem. Commun.*, 2019, DOI: 10.1039/C8CC10069A.



This is an Accepted Manuscript, which has been through the Royal Society of Chemistry peer review process and has been accepted for publication.

Accepted Manuscripts are published online shortly after acceptance, before technical editing, formatting and proof reading. Using this free service, authors can make their results available to the community, in citable form, before we publish the edited article. We will replace this Accepted Manuscript with the edited and formatted Advance Article as soon as it is available.

You can find more information about Accepted Manuscripts in the [author guidelines](#).

Please note that technical editing may introduce minor changes to the text and/or graphics, which may alter content. The journal's standard [Terms & Conditions](#) and the ethical guidelines, outlined in our [author and reviewer resource centre](#), still apply. In no event shall the Royal Society of Chemistry be held responsible for any errors or omissions in this Accepted Manuscript or any consequences arising from the use of any information it contains.

Journal Name

COMMUNICATION

Mechanised Lubricating Silica Nanoparticles for On-Command Cargo Release on Simulated Surface of Joint Cavity

Xiaolong Tan,^{†a} Yulong Sun,^{†a} Tao Sun^a and Hongyu Zhang^{*a}Received 00th January 20xx,
Accepted 00th January 20xx

DOI: 10.1039/x0xx00000x

www.rsc.org/

We describe a type of supramolecular host-guest functioned silica nanoparticles activated by energy conversion from the joint movement. High coefficient of friction from damaged joints causes more energy conversion to weaken the surface host-guest interaction, resulting in target cargo release. Additionally, the hydrated layer on the nanoparticle surface plays a role in lubrication enhancement.

Mechanised silica nanoparticles (MSNs) have been paid much attention in the last two decades.¹ Three significant elements are involved in these systems, including (i) porous materials, like mesoporous silica nanoparticles,² as nanocontainers; (ii) switchable interlocked molecules (SIM) as stoppers such as rotaxanes and pseudorotaxanes;^{3,4} and (iii) extra activation methods such as light,⁵⁻⁷ pH value,⁸⁻¹² heat,¹²⁻¹⁴ reduce-oxide,¹⁵ and enzyme¹⁶ activations. To achieve the purposes of controlled release, SIMs are installed on the surface of MSNs, which will generate the nanoscale movement in the suitable activations. The first MSNs was raised in 2004,¹⁷ which showed the effectively controlled release properties of organic dye. However, the performance of release has been limited as it could only work in an organic solvent. From 2007, the design of the surface SIMs has been replaced by water-soluble macrocycles, such as cyclodextrin and cucurbituril.¹⁸⁻²¹ The release properties in water showed the potential of biological controlled release. In 2012, a light-activated MSNs was prepared and performed in biological media, which raised the meaning of targeting release.⁷ In the last several years, different kinds of activation methods and loading containers have been used and made a good stage on the detection and treatment of cancer and other diseases.^{22, 23} However, the cartilage structure of the joint cavity tends to be relatively closed, the common

activation could not be applied in joint cavity.^{24, 25} Therefore, herein we propose a release system, combining the properties of the cartilage tissues. In this design, we use the heat energy, which is converted from the movement of joints. The increase in temperature can lower the binding constant of the surface inclusion complex.²⁶ Thereby the design can be stimulated to release the drug locally. More importantly, the damage to the surface of the joint cavity, like osteoarthritis, leads to an increase of coefficient of friction (COF). Therefore, in the pathological joint movement, more mechanical energy will convert to heat, which results in a significant rise in drug release. At the same time, highly charged molecules are assembled on the surface of the nanoparticles, which form hydration layers, thus improving the lubrication property.²⁷ The local release of anti-inflammatory drug and lubrication enhancement are both desired for osteoarthritis treatment.

The fabrication activation approaches of the MSNs are depicted in Fig. 1 and ESI. Betaines (chemical structure in Fig. 1) are installed on the surface of aminated silica nanoparticles (MSNs-

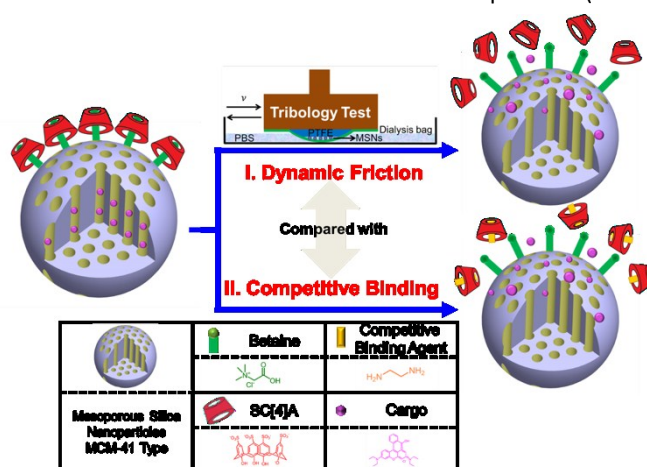


Fig.1 Illustration of friction-controlled mechanized drug delivery system. Two types of activations, (a) dynamic friction, (b) competitive binding, are applied in this system.

^a State Key Laboratory of Tribology, Department of Mechanical Engineering, Tsinghua University, Beijing 100084, P. R. China.

[†] These authors contributed equally to this work.

Electronic Supplementary Information (ESI) available: materials preparation and characterisations, tribological test, controlled release experiments, simulations, and in vitro cytotoxicity. See DOI: 10.1039/x0xx00000x

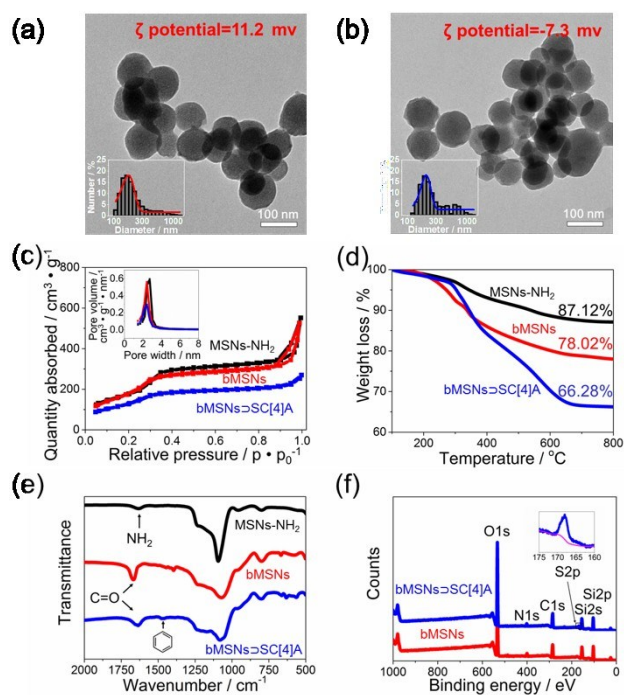


Fig. 2 Morphological, thermodynamic, and spectroscopic characterisations of bMSNs@SC[4]A, compared with MSNs-NH₂ and bMSNs: TEM images of (a) bMSNs (distribution of diameter size in the bottom left corner and zeta potential in the top right corner) and (b) bMSNs@SC[4]A (distribution of diameter size in the bottom left corner and zeta potential in the top right corner); (c) N₂ adsorption-desorption isotherm (pore size distribution in the top left corner) of MSNs-NH₂ (black), bMSNs (red), and bMSNs@SC[4]A (blue); (d) TGA curves of MSNs-NH₂ (black), bMSNs (red), and bMSNs@SC[4]A (blue); (e) FT-IR spectra of MSNs-NH₂ (black), bMSNs (red), and bMSNs@SC[4]A (blue); (f) XPS spectra of bMSNs (red) and bMSNs@SC[4]A (blue).

NH₂). After loading model cargoes, Rhodamine B (RhB), p-sulfonato-calix[4]arenes (SC[4]A) self-assembles with betaine-modified MSNs (bMSNs) to form the host-guest complex (Binding Constant: $\log K = 4.9$)²⁸ and control the loaded cargoes out of the nanocontainers (bMSNs@SC[4]A@RhB). The controlled cargo release is achieved by dynamic friction and competitive binding. Compared with other activations, dynamic friction with coherent and periodic process simulates the motion of bone joints, which provides a huge contribution to the drug delivery of joint cartilage structure. Besides, SC[4]A introduces a large number of charges which can assist a tenacious hydration layer to reduce the friction and wear of bone joints and enhance the lubricating properties of the surface. Most importantly, we investigate the mechanism of friction-controlled release and propose the potential lubrication mechanism, which offers an important basis for further designs.

Morphological, thermodynamic, and spectroscopic characterisations of bMSNs@SC[4]A, compared with MSNs-NH₂ and bMSNs, are shown in Fig. 2. TEM images (Fig. 2a and 2b) show the sizes before and after modification are around 100 nm.

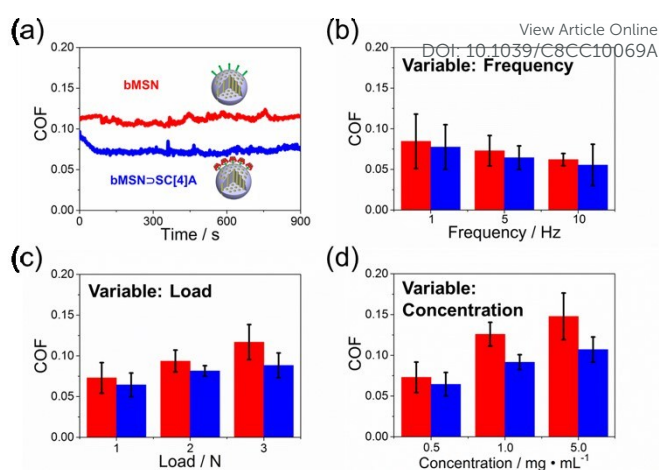


Fig. 3 The aqueous lubrication properties of bMSNs@SC[4]A (blue) compared with bMSNs (red) by using UMT: (a) COF-time plots (reciprocating frequency: 2 Hz; applied load: 3 N; concentration: 1.0 mg/mL); (b) comparison of the COF under different reciprocating frequencies (concentration: 0.5 mg/mL; applied load: 1 N); (c) comparison of the COF under different reciprocating loads (concentration: 0.5 mg/mL; reciprocating frequency: 5 Hz); (d) comparison of the COF at different concentrations of materials (applied load: 1 N; reciprocating frequency: 5 Hz).

There is no visible difference in size, which proves the modification approach does not destroy the structure of the materials. Additionally, the size distributions from dynamic light scattering (DLS) increase because of the formation of hydrated layers, which is displayed in ESI. The mesostructures of MSNs are carried out by using BET (Fig. 2c). Combining with the ordered uniform pores from TEM, we confirm all the MSNs we use is MCM-41 type.² More details of pore size distribution by three methods are tested and calculated in Fig. 2c and ESI. TGA curves (Fig. 2d) display the increase of weight loss proving the successful preparations of both betaine modification and SC[4]A self-assembly on the surface of MSNs. From FT-IR spectra (Fig. 2e), a new peak formed at 1634 cm⁻¹, corresponding to the C=O stretching vibration of amides, indicates betaine molecules have been modified on the surface of MSNs-NH₂. The self-assembly step does not form any new chemical bonds. However, we observe the benzene-based skeleton vibration from SC[4]A, which is located at 1458 cm⁻¹. Further evidence of self-assembly in Fig. 2f is provided by using X-ray photoelectron spectra (XPS) due to the new peak belonging to SC[4]A (More detailed discussion of this section is shown in ESI).

The lubrication properties of both bMSNs and bMSNs@SC[4]A are evaluated by using Universal Micro-Tribology (UMT) in Fig. 3. Overall, the COF is reduced after the assembly of SC[4]As to the surface of bMSNs. Fig. 3a shows a high-intensity continuous friction experiment to investigate the total friction properties. The friction curve of bMSNs@SC[4]A is much smoother than before assembly of SC[4]As, which shows the stable lubricating properties of bMSNs@SC[4]A. According to the hydration

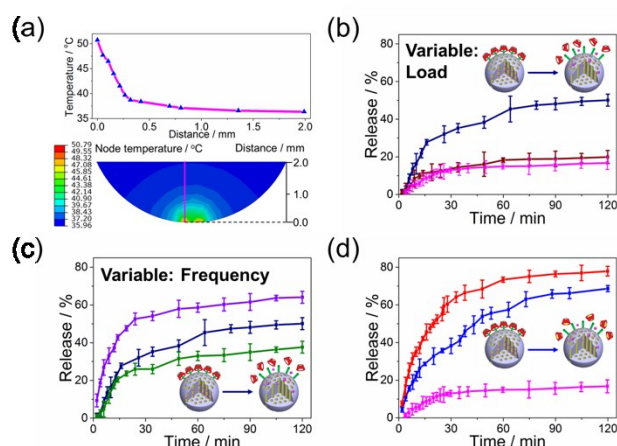


Fig. 4 Controlled release profiles of bMSNs@SC[4]A@RhB: (a) numerical simulation of energy conversion by ABAQUS including temperature distribution curve of the distance from the contact area (upper) and temperature distribution of center longitudinal section of the simulated movement surface (lower); (b) release curves of bMSNs@SC[4]A@RhB with 2 Hz dynamic friction of different loads: 0 N (pink), 1 N (wine) and 4 N (navy); (c) release curves of bMSNs@SC[4]A@RhB with 4 N loaded dynamic friction of different frequencies: 1 Hz (green), 2 Hz (navy), and 3 Hz (purple); (d) release curves of competitive binding (binding agent: 2 mL ethylenediamine, blue), compared with the release curve of bMSNs@RhB (red) and bMSNs@SC[4]A@RhB without any activation (pink).

lubrication mechanism,²⁷ SC[4]A molecules attract more charges onto the surface of bMSNs to form a tenacious hydrated layer, which improves the lubrication performance. To further determine the lubrication mechanism of bMSNs and bMSNs@SC[4]A, we also test the COFs with different frequencies, loads, and concentrations. Generally, there is only a slight difference among various conditions, especially the tests in frequencies and loads. Although we discover a relatively apparent increasing of COF with different concentrations, it is related with the abrasive effect of MSNs.²⁵ Therefore, we propose the lubrication mechanism of this system is boundary lubrication according to the Stribeck curve (More details about lubrication states are shown in ESI).

The release profiles and mechanism of bMSNs@SC[4]A@RhB with dynamic friction are examined, compared with the release of competitive binding (Fig. 4). The energy conversion during dynamic friction between the surfaces of the joint cavity is simulated and shown in Fig. 4a. Parts of the generated mechanical energy converted into heat, which leads to a significant increase in temperature at the contact area. After a reciprocating movement of 4.5 s, local temperature at contact area raises to 50.79 °C (More details in ESI). Due to the increase in contact temperature, a significant entropy increase occurs on the surface of the material. The mounting surface chaos directly impairs the ion-dipole interaction of the inclusion complex,²⁶ thereby releasing the molecules out of the inorganic container. The speed of the generation of energy, corresponding to the accumulation of temperature, depends mainly on the load and

sliding frequency. Therefore, different conditions are employed to investigate the cargo release property under different loads (Fig. 4b) and sliding frequencies (Fig. 4c). The cargo release profiles with no dynamic friction and load of 1 N show a similar tendency, only a limited cargo (less than 20%) is released after 120 min. Nevertheless, bMSNs@SC[4]A@RhB are effectively activated under the load of 4 N, with a total cargo release reaching 50% after 120 min. It indicates that the host-guest interaction between SC[4]A and betaine could not be weakened under mild load (1 N). But under severe friction (4 N), the increase of temperature leads to the destruction of the host-guest interaction, resulting in an obvious cargo release. Apparently, the higher the sliding frequency is, the faster the temperature accumulates and the quicker the cargo releases. In addition, the cargo release properties of bMSNs@RhB and bMSNs@SC[4]A@RhB with a competitive binding agent is performed by adding ethylenediamine (Fig. 4d). Compared with the competitive binding approach, the release performance of dynamic friction is much gentler and more controllable, thereby enhancing the efficiency and availability of loading cargoes.

In conclusion, the smart release system, bMSNs@SC[4]A, is successfully applied and activated by the movement of simulated bone joints. The inclusion complexes on the surface not only control the release of the cargoes but also reduce the friction and wear of the joint surface. The mechanism of release is mainly due to the conversion of mechanical energy into heat during the friction process. The hydrated lubrication layer formed by the highly charged structure of the surface significantly reduces the COF, thereby improving the friction and wear properties of the surface. As the friction conditions changed, the COF does not change significantly, and the lubrication mechanism conforms to boundary lubrication. In addition, we have made appropriate evaluations on the toxicity and biocompatibility of bMSNs@SC[4]A (More details in ESI), thus demonstrating the biological application prospects of the smart release system in the future.

This study is financially supported by National Natural Science Foundation of China (Grant no. 51675296), Ng Teng Fong Charitable Foundation (Grant No. 202-276-132-13), Tsinghua University Initiative Scientific Research Program (Grant no. 20151080366), and Research Fund of State Key Laboratory of Tribology, Tsinghua University, China (Grant no. SKLT2018B08).

Conflicts of interest

There are no conflicts to declare.

Notes and references

- Z. Li, J. C. Barnes, A. Bosoy, J. F. Stoddart and J. I. Zink, *Chem. Soc. Rev.*, 2012, 41, 2590–2605.
- J. S. Beck, J. C. Vartuli, W. J. Roth, M. E. Leonowicz, C. T. Kresge, K. D. Schnitt, C.-T. W. Chu, D. H. Olson, E. W. Sheppard, S. B. McCullen, J. B. Higgins and J. L. Schlenker, *J. Am. Chem. Soc.*, 1992, 114, 10834–10843.

- 3 Y. Sun, Y. Yang, D. Chen, G. Wang, Y. Zhou, C. Wang and J. F. Stoddart, *Small*, 2013, **9**, 3224–3229.
- 4 M. Li, H. Yan, C. Teh, V. Korzh and Y. Zhao, *Chem. Commun.*, 2014, **50**, 9745–9747.
- 5 A. Agostini, F. Sancenón, R. Martínez-Mañez, M. D. Marcos, J. Soto and P. Amoros, *Chem.–Eur. J.*, 2012, **18**, 12218–12221.
- 6 D. P. Ferris, Y. Zhao, N. M. Khashab, H. A. Khatib, J. F. Stoddart and J. I. Zink, *J. Am. Chem. Soc.*, 2009, **131**, 1686–1688.
- 7 Y. Sun, B. Yang, S. X. Zhang and Y. Yang, *Chem.–Eur. J.*, 2012, **18**, 9212–9216.
- 8 S. Wu, X. Huang and X. Du, *Angew. Chem. Int. Ed.*, 2013, **52**, 5580–5584.
- 9 F. Muhammad, M. Guo, W. Qi, F. Sun, A. Wang, Y. Guo and G. Zhu, *J. Am. Chem. Soc.*, 2011, **133**, 8778–8781.
- 10 T. Chen, N. Yang and J. Fu, *Chem. Commun.*, 2013, **49**, 6555–6557.
- 11 B. Li, Z. Meng, Q. Li, X. Huang, Z. Kang, H. Dong, J. Chen, J. Sun, Y. Dong, J. Li, X. Jia, J. L. Sessler, Q. Meng and C. Li, *Chem. Sci.*, 2017, **8**, 4458–4464.
- 12 X. Huang, S. Wu, X. Ke, X. Li and X. Du, *Appl. Mater. Interfaces*, 2017, **9**, 19638–19645.
- 13 D. De and G. M. Mandal, *Biomicrofluidics*, 2016, **10**, 064112.
- 14 N. John and S. George, *J. Drug. Deliv. Sci. Tec.*, 2018, **46**, 294–301.
- 15 D. Guo, S. Chen, H. Qian, H. Zhang and Y. Liu, *Chem. Commun.*, 2010, **46**, 2620–2622.
- 16 Y. Sun, Y. Zhou, Q. Li and Y. Yang, *Chem. Commun.*, 2013, **49**, 9033–9035.
- 17 R. Hernandez, H. R. Tseng, J. W. Wong, J. F. Stoddart and J. I. Zink, *J. Am. Chem. Soc.*, 2004, **126**, 3370–3371.
- 18 C. Park, K. Oh, S. C. Lee and C. Kim, *Angew. Chem. Int. Ed.*, 2007, **46**, 1455–1457.
- 19 S. Angelos, Y. Yang, K. Patel, J. F. Stoddart and J. I. Zink, *Angew. Chem., Int. Ed.*, 2008, **47**, 2222–2226.
- 20 K. Patel, S. Angelos, W. R. Dichtel, A. Coskun, Y. Yang, J. I. Zink and J. F. Stoddart, *J. Am. Chem. Soc.*, 2008, **130**, 2382–2383.
- 21 K. M. Park, K. Suh, H. Jung, D. W. Lee, Y. Ahn, J. Kim, K. Baek and K. Kim, *Chem. Commun.*, 2008, **1**, 71–73.
- 22 M. Liong, S. Angelos, E. Choi, K. Patel, J. F. Stoddart and J. I. Zink, *J. Mater. Chem.*, 2009, **19**, 6251–6257.
- 23 Y. Yan, T. Sun, H. Zhang, X. Ji, Y. Sun, X. Zhao, L. Deng, J. Qi, W. Cui, H. A. Santos and H. Zhang, *Adv. Funct. Mater.* 2018, 10.1002/adfm.201807559
- 24 S. Jahn, J. Seror and J. Klein, *Biomed. Eng.*, 2016, **18**, 235–258.
- 25 T. Sun, Y. Sun and H. Zhang, *Polymers*, 2018, **10**, 513–522.
- 26 Y. Luo and F. J. Millero, *Geochim. Cosmochim. Ac.*, 2007, **71**, 326–334.
- 27 The mechanism of hydration lubrication is converting the friction objectives from the two inorganic surfaces to water film between surfaces. The charged materials can form a strong interaction with water molecules by ion-dipole interactions and hydrogen bond. Therefore, the friction happens between water films which show an extremely low friction coefficient. See: J. Klein, *Friction*, 2013, **1**, 1–23.
- 28 J. M. Lehn, R. Meric, J. P. Vigneron, M. Cesario, J. Guilhem, C. Pascard, Z. Asfari and J. Vicens, *Supramol. Chem.*, 1993, **5**, 97–103.

View Article Online
DOI: 10.1039/C8CC10069A